Available online at www.sciencedirect.com
SCIENCE DIRECT
ELSEVIER
Journal of the European Ceramic Society 26 (2006) 2833–2837
ECERS
www.elsevier.com/locate/jeurceramsoc

X-ray diffraction and infrared spectra studies of $Fe_xMn_{2.34-x}Ni_{0.66}O_4$ ($0<x<1$) NTC ceramics

Zhongbing Wang [a], Chunhua Zhao [a], Pinghua Yang [a], A.J.A. Winnubst [a,b], Chusheng Chen [a,*]

[a] *Department of Material Science and Engineering, University of Science and Technology of China, Hefei, Anhui 230026, China*
[b] *Laboratory for Inorganic Materials Science, Faculty of Science and Technology & MESA+ Institute for Nanotechnology, University of Twente, P.O. Box 217, 7500 AE Enschede, The Netherlands*

Received 30 January 2005; received in revised form 26 April 2005; accepted 15 May 2005
Available online 25 July 2005

Abstract

Series of $Fe_xMn_{2.34-x}Ni_{0.66}O_4$ ($0<x<1$) NTC ceramics were prepared by the Pechini method. Resistivity, thermal constant (B) and aging values were measured. It was found that the resistivity increased with increasing iron content x. The B value however first decreased with increasing x in the range of $x<0.6$ and then increased with further increase in x. Aging reached a maximum in the middle range ($x=0.4$–0.6) of iron content. X-ray diffraction (XRD) and infrared analysis were used to determine the distribution of Fe^{3+} ions. The Fe^{3+} ions were found to occupy both A- and B-site when $x<0.6$ and then go to B-site when $x>0.6$. An redistribution of the Fe^{3+} ions between A- and B-site was related to the aging of the NTC thermistor.

Keyword: Spinels; X-ray methods; Thermistor

1. Introduction

Negative temperature coefficient (NTC) ceramic thermistors are increasingly used in various industrial and domestic applications, such as elements for the suppression of in-rush current, for temperature measurement and control, and for the compensation of other circuit elements. The specific resistivity of these ceramics follows the well known Arrhenius relation: $\rho=\rho_0\exp(E_a/kT)$, in which ρ is the specific resistivity; E_a is the activation energy for conduction; k, the Boltzmann's constant and T, the absolute temperature.[1] In practice, the NTC thermistors are characterized by two parameters, B, the thermal constant (unit in Kelvin) which is related to $B=E_a/k$, and $\rho_{25\,^\circ C}$, the specific resistivity at 25 °C.

The NTC ceramics often consist of 3d transition metal oxides, such as Mn-Ni-oxide,[2] Mn-Ni-Co-oxide,[3] Mn-Ni-Fe-oxide, etc.[4] with the spinel structure of the general formula AB_2O_4. In this structure there are two sites available for the cations, a tetrahedral site, A-site, and an octahedral site, B-site.[5] For Fe–Mn–Ni–O system, Mn^{3+}, Mn^{4+} and Ni^{2+} ions prefer to occupy the B-site, and Mn^{2+} ions tends to reside at the A-site. As to Fe^{3+} ions, the situation is more complicated, as Fe^{3+} ions can go to A-site as well as B-site.[6] Methods used in literature to study the cations distribution include X-ray diffraction (XRD),[7] neutron diffraction[8] and Mössbauer spectroscopy, etc.[9] Besides these methods, infrared (IR) spectroscopy may also be used to investigate the cation distribution in spinel. In the study of IR spectra of ferrite spinels by Waldron[10] half a century ago, on the basis of the group theory, four IR active modes were identified, which were marked ν_1, ν_2, ν_3 and ν_4 from high frequency to low frequency, ν_1 and ν_2 are assigned to tetrahedral and octahedral group complexes respectively. However, in a subsequent study by Preudhomme,[11] ν_1 and ν_2 are attributed to vibrations of the lattice of octahedral groups for II–III normal spinel.

* Corresponding author. Fax: +86 551 3601592.
E-mail address: ccsm@ustc.edu.cn (C. Chen).

0955-2219/$ – see front matter © 2005 Elsevier Ltd. All rights reserved.
doi:10.1016/j.jeurceramsoc.2005.05.007

The electrical properties of spinel NTC ceramics have been found to be largely affected by the distribution of the cations. Electrical conductivity is generally believed to occur via the electron jumping between Mn^{3+} and Mn^{4+} ions at the B-site.[12] A drift in resistivity of the NTC ceramics with time, termed aging, is also believed to arise from the redistribution of the cations between the A- and B-site.[13] In the present paper, the Fe^{3+} ions distribution in $Fe_xMn_{2.34-x}Ni_{0.66}O_4$ ($0<x<1$) series was studied on fresh and aged powder samples using XRD and IR and correlated with the electrical properties.

2. Experimental

The Pechini method was used to prepare $Fe_xMn_{2.34-x}Ni_{0.66}O_4$ ($x=0$, 0.15, 0.3, 0.4, 0.6, 0.8, 1.0). Appropriate amounts of $Fe(NO_3)_3$, $Ni(NO_3)_2$, $Mn(NO_3)_2$ were dissolved in deionized water. Citric acid (CA) and ethyl glycol (EG) were added to the solution with a molar ratio [Fe + Mn + Ni]:CA:EG = 1:2:2. The pH of the solution was adjusted to about 3 with ammonia. The solution was heated first at 90 °C under stirring to form a more viscous solution and then heated to 140 °C for esterfication resulting in the formation of a resin. Upon further heating at elevated temperatures on a hot plate, spontaneous ignition of the resin occurred, resulting in a fluffy ash. The ash was milled in ethanol for 24 h, dried at 75 °C, and then calcined at 700 °C for 4 h. The calcined powders were milled in ethanol, dried, blended with an organic binder (PVA, $n=1750$, Supplied by Shanghai Chemical Reagent Co. Ltd., China), sieved and were uniaxially pressed at 60 MPa into disks with a diameter of 6 mm and a thickness of 2 mm and then isostatically pressed at 300 MPa. The disks were heated in air to 400 °C at a rate of 100 °C/h and kept at that temperature for 2 h to remove the organic binder, and then heated to 1200 °C at a rate of 250 °C/h and kept at that temperature for 10 h for sintering, and furnace-cooled to room temperature. The density ρ was measured using Archimedes method, the relative density ρ_{rel} was determined according to the formula $\rho_{rel}=\rho/\rho_{th}$, where ρ_{th} is the theoretical density calculated from the lattice parameters as obtained from X-ray diffraction data.

Sintered samples were crushed and subsequently powder XRD measurements were performed using a PHILIPS X'Pert diffractometer (Cu Kα) with a step size of 0.0167° and 2θ range from 15° to 75°. Lattice parameters were fitted using Powdercell software by the least squares method.[14] IR spectra on the crushed samples were recorded on a Bruker VECTOR-22 spectrometer in KBr medium. For electrical resistance measurements, the two opposite sides of the sintered disks were polished and coated with silver paste, and heated at 850 °C for 15 min for metallization and quenched to room temperature. Silver wires were attached as electrode leads. The electrical resistances were measured in an oil bath at 25 and 50 °C by a two-probe technique with an Agilent34401A digital multimeter. The thermal constant B was calculated according to the formula $B=3853.89\ln(R_{25}/R_{50})$, in which R_{25} and R_{50} are resistances at 25 and 50 °C, respectively. Aging of the specimens was performed in a furnace at 150 °C in air for 1000 h. Aging is defined by $\Delta R/R_0=(R-R_0)/R_0$, in which R_0 is the resistivity at 25 °C before the aging test, and R is the resistivity at 25 °C after aging at 150 °C for 1000 h in air. The values of the specific resistivity, B value and aging value average for three specimens.

3. Results and discussion

3.1. Microstructure and electrical properties of as-prepared samples

A typical XRD pattern of the $x=0.4$ specimen after sintering and subsequent crushing is given in Fig. 1. From the lattice parameters as presented in Fig. 2, it can be seen that the values decrease with increasing iron content. This is due

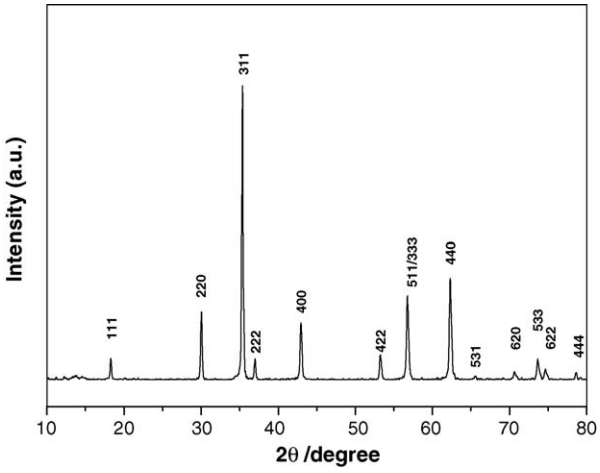

Fig. 1. X-ray diffraction pattern for the $Fe_{0.4}Mn_{0.94}Ni_{0.66}O_4$.

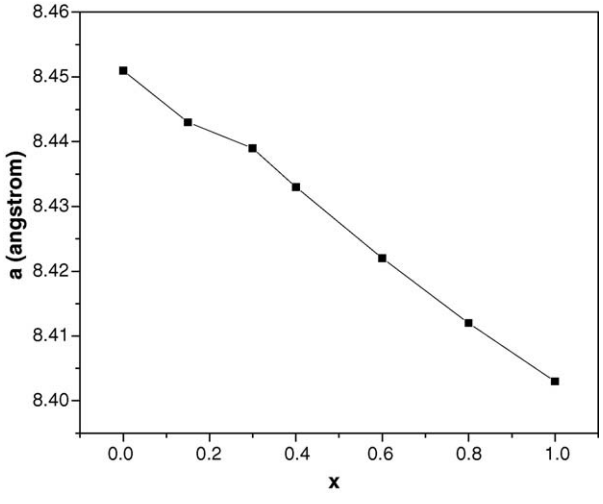

Fig. 2. Lattice parameter for the $Fe_xMn_{2.34-x}Ni_{0.66}O_4$ series ($0<x<1$).

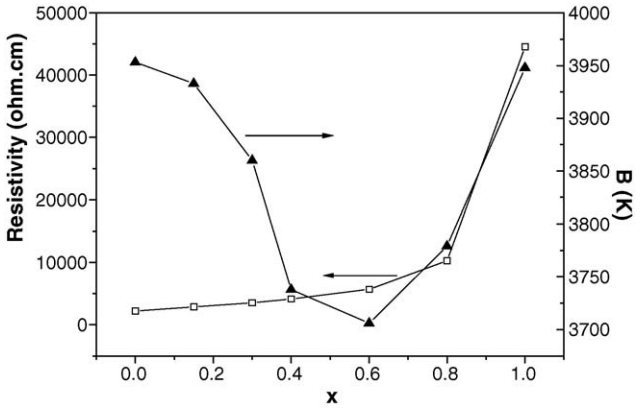

Fig. 3. Resistivity and B value for the $Fe_xMn_{2.34-x}Ni_{0.66}O_4$ series as a function of iron content, x.

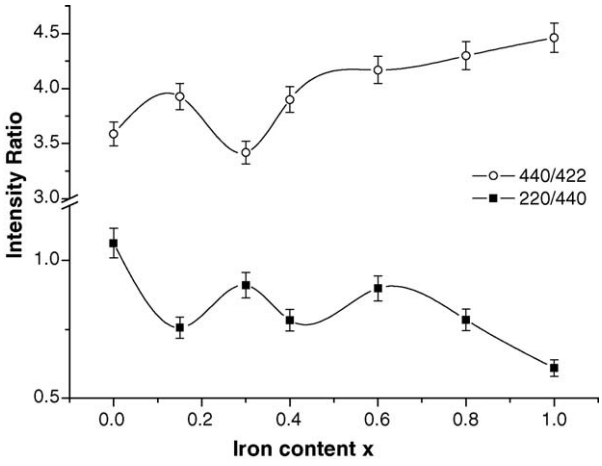

Fig. 4. Variation of X-ray intensity ratios (I_{220}/I_{400}) and (I_{440}/I_{422}) with iron content, x.

to the smaller radius of Fe^{3+} (0.55 Å) if compared with Mn^{3+} (0.58 Å). The XRD patterns of the $Fe_xMn_{2.34-x}Ni_{0.66}O_4$ series indicate that all specimens are of the single cubic spinel structure. After sintering all samples had a relative density of about 95%.

Fig. 3 shows the specific resistivity at 25 °C and B values of the $Fe_xMn_{2.34-x}Ni_{0.66}O_4$ series. As can be seen from Fig. 3, the resistivity first increases slightly with increasing iron content at $x<0.6$ and then sharply in the range of $x>0.6$, while the B value first decreases for $x<0.6$ and increases afterwards. It is known that electrical conduction in these spinels is via hopping of electrons between the Mn^{3+} and Mn^{4+} ions present at the octahedral sites.[12] The increase in iron content leads to a decrease in $[Mn^{3+}]$ and $[Mn^{4+}]$ and thus an increase in resistivity. In general, for NTC thermistors, a higher resistivity corresponds to a higher B value.[6] However, this does not hold for the $Fe_xMn_{2.34-x}Ni_{0.66}O_4$ series in the range of $x<0.6$ where with increasing x resistivity increases slightly whereas B decreases (see Fig. 3). This decrease in B for $x<0.6$ may be attributed to the Jahn–Teller effect of Mn^{3+} ions that results in distorted MnO_6 octahedrons and thus makes electron hopping between Mn^{3+} and Mn^{4+} ions more difficult. For $x>0.6$, the Jahn–Teller effect of Mn^{3+} ions becomes less severe, thus both resistivity and B value change consistently.

It is known that the intensities of the (220), (440) and (422) XRD reflections is closely related to the distribution of cations in a spinel.[15] Fig. 4 shows the intensity ratios I_{220}/I_{440} and I_{440}/I_{422} for the $Fe_xMn_{2.46-x}Ni_{0.54}O_4$ series. When $x<0.6$, both I_{220}/I_{440} and I_{440}/I_{422} fluctuate with variation of iron content, and an increase (decrease) in I_{220}/I_{440} always corresponds to a decrease (increase) in I_{440}/I_{422}. As to $x>0.6$, with increasing x, I_{220}/I_{440} decreases whereas I_{440}/I_{422} increases.

The XRD intensity, in principle, can be calculated using the formula suggested by Buerger[16]: $I_{hkl}=|F_{hkl}|^2PL_PTA$, where I_{hkl} is the integrated intensity; F_{hkl}, the structure factor; P, the multiplicity factor for the plane (hkl) and L_P the Lorentz polarization factor, $L_P=(1+\cos^2 2\theta)/(\sin^2\theta\cos\theta)$. In calculating the intensity ratios of the peaks, the absorption factor (A) and temperature (T) need not to be taken into account. For $Fe_xMn_{2.46-x}Ni_{0.54}O_4$ series with the same space group, the intensity ratio of the peaks is simply determined by the structure factor F_{hkl} which in turn is determined by the distribution of the cations. With the assistance of the Powdercell software[14] one can examine how the intensity ratio of the peaks is affected by the cation distribution in the AB_2O_4 spinel. It shows that when more heavy ions enter the A-site, the intensity ratio I_{220}/I_{440} increases whereas I_{440}/I_{422} decreases. But, when the B-site is occupied by more heavy ions, I_{220}/I_{440} decreases whereas I_{440}/I_{422} increases. In comparison with the data shown in Fig. 4, it becomes clear that Fe^{3+} ions which are heavier than the Ni^{2+} ions tend to occupy both the A- and B-site in the range of iron content $x<0.6$. But for the composition $x>0.6$, the newly added Fe^{3+} ions preferentially occupy the B-site, as revealed by the decrease in I_{220}/I_{440} and increase in I_{440}/I_{422}. The change in the occupation of Fe^{3+} ions in the spinel may account for the variation of the electrical resistivity. The electrical resistivity for the composition $x<0.6$ is less sensitive to the change in the Fe^{3+} ion content because not all Fe^{3+} ions occupy B-site, thus the network of Mn^{3+} and Mn^{4+} responsible for electrical conduction is less interrupted. But, for the composition $x>0.6$, Fe^{3+} ions mainly go to B-site, thus has much stronger effect on the resistivity.

The room temperature infrared absorption spectra of the investigated powder samples were also measured. The wave numbers ν_1 and ν_2 are listed in Table 1. It can be seen that ν_2 decreases significantly with increasing iron content x, whereas ν_1 decreases slightly for $x<0.6$ and almost levels off at higher x values. According to Waldron's results, ν_1 and ν_2 are assigned to vibrations of tetrahedral and octahedral complexes respectively. Since the crystal structure and metal ion valence remain unchanged for the whole series of $Fe_xMn_{2.46-x}Ni_{0.54}O_4$ ($x=0.0-1.0$), the change in wave number ν can be related to a change in A- and B-site occupation of metal ions of different mass. The replacement of Mn by Fe leads to the decrease in wave number, since the

Table 1
Vibration frequencies of the $Fe_xMn_{2.34-x}Ni_{0.66}O_4$ series

	ν_1 (cm^{-1})	ν_2 (cm^{-1})
$x=0$	597.2	473.3
$x=0.15$	593.7	461.6
$x=0.3$	591.7	445.9
$x=0.4$	591.5	443.2
$x=0.6$	590.2	438.1
$x=0.8$	591.0	426.0
$x=1.0$	589.0	427.6

atomic weight of Fe is higher than that of Mn. The changes in ν_1 and ν_2 with iron content x again suggest that Fe^{3+} ions occupy both A- and B-site in the range of $x<0.6$; for $x>0.6$ the number of Fe^{3+} ions at the B-site increases with increasing x while the amount of Fe^{3+} ions at the A-site remains unchanged. Fig. 5 shows some typical IR spectra. It can be seen that the IR signals become broader with increasing iron content x, which may be attributed to the existence of more multi-cations at both A- and B-site.

3.2. Aged samples

The aging values ($\Delta R/R_0$) of the $Fe_xMn_{2.34-x}Ni_{0.66}O_4$ series after heat treatment at 150 °C for 1000 h are shown in Fig. 6. The aging values are very dependent on iron content. The aging is small at both low and high iron content and large in the middle range of $x=0.4$–0.6. This trend is consistent with that of $Fe_xMn_{2.46-x}Ni_{0.54}O_4$ series.[6] The aged samples also show some change in the intensity ratio of XRD peaks. For comparison, the XRD patterns for samples $x=0.4$ and $x=0.8$ were examined. The integral area of the peaks 220 and 440 were calculated for both fresh and aged specimens. After aging, the I_{220}/I_{440} value changes from 0.83 to 0.91 for sample $x=0.4$, increasing by 9.6%. However, the intensity ratio changes from 0.82 to 0.84 for sample $x=0.8$, an increase of only 2.4%. A strong increase in I_{220}/I_{440} for $x=0.4$ reveals that heat treatment at elevated temperature of 150 °C results

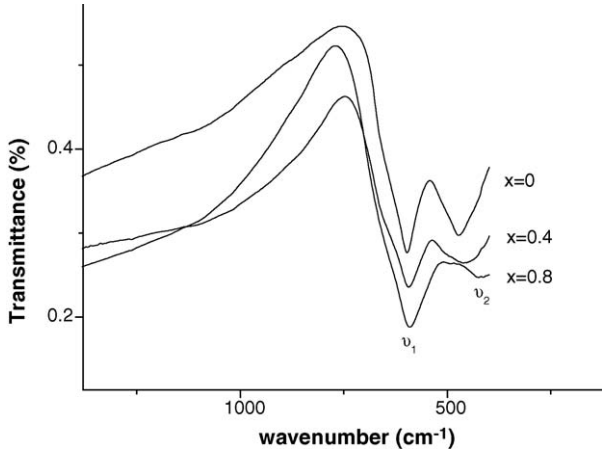

Fig. 5. Some typical IR spectra of the $Fe_xMn_{2.34-x}Ni_{0.66}O_4$ for $x=0$, 0.4, 0.8.

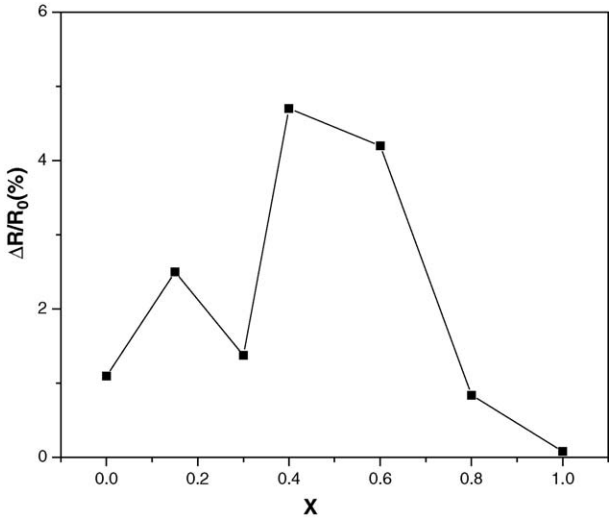

Fig. 6. Relative change in resistivity for $Fe_xMn_{2.34-x}Ni_{0.66}O_4$ samples after aging at 150 °C for 1000 h.

in migration of heavy ions (i.e. Fe^{3+} ions) from the B- to the A-site and thus a higher aging.

4. Conclusions

$Fe_xMn_{2.46-x}Ni_{0.54}O_4$ ($0<x<1$) series NTC ceramics can be prepared using the Pechini method. The resistivity increases with increasing iron content, whereas the thermal constant B decreases first in the range of $x<0.6$ and then increases for $x>0.6$. The aging is large in the middle range ($x=0.4$–0.6) of iron content and small at low and high iron contents. Both XRD and IR analysis suggest that Fe^{3+} ions first go to both the A- and B-site in the range of $x<0.6$; and then preferentially go to B-site for $x>0.6$. The migration of Fe^{3+} ions from the B- to the A-site is responsible for aging of the NTC thermistor.

References

1. Rousset, A., Legros, R. and Lagrange, A., Recent progress in the fabrication of ceramic negative temperature coefficient thermistors. *J. Eur. Ceram. Soc.*, 1994, **13**, 185–189.
2. Fritsch, S., Sarrias, J., Brieu, M. *et al.*, Correlation between the tructure, the microstructure and the electrical properties of nickel manganite negative temperature coefficient (NTC) thermistors. *Solid State Ionics*, 1998, **109**, 229–237.
3. Hosseini, M., The effect of cation composition on the electrical properties and aging of Mn–Co–Ni thermistors. *Ceram. Int.*, 2000, **26**, 245–249.
4. Feltz, A. and Pölzl, W., Spinel forming ceramics of the system $Fe_xNi_yMn_{3-x-y}O_4$ for high temperature NTC thermistor applications. *J. Eur. Ceram. Soc.*, 2000, **20**, 2353–2366.
5. Sickafus, K. E., Wills, J. M. *et al.*, Structure of spinel. *J. Am. Ceram. Soc.*, 1999, **82**, 3279–3292.
6. Groen, W. A., Metzmacher, C., Huppertz, P. and Schuurman, S., Aging of NTC ceramics in the system Mn–Ni–Fe–O. *J. Electroceram.*, 2001, **7**, 77–87.

7. Baltzer, P. K. and White, J. G., Crystallographic and magnetic studies of the system $(NiFe_2O_4)_{1-x} + (NiMn_2O_4)_x$. *J. Appl. Phys.*, 1958, **29**, 445–447.
8. Hastings, J. M. and Corliss, L. M., Neutron diffraction study of manganese ferrite. *Phys. Rev.*, 1961, **104**, 328–331.
9. Battault, T., Legros, R. and Rousset, A., Structure and electrical properties of iron manganite spinels in relation with cationic distribution. *J. Eur. Ceram. Soc.*, 1995, **15**, 1141–1147.
10. Waldron, R. D., Infrared spectrum of ferrites. *Phys. Rev.*, 1955, **99**, 1727–1735.
11. Preudhomme, J. and Tarte, P., Infrared studies of spinels-III: the normal II–III spinels. *Spectrochim. Acta*, 1971, **27A**, 1817–1835.
12. Macklen, E. D., Electrical conductivity and cation distribution in nickel manganite. *J. Phys. Chem. Solids*, 1986, **47**, 1073–1079.
13. Battault, T., Legros, R. and Rousset, A., Aging of iron manganite negative temperature coefficient thermistors. *J. Mater. Res.*, 1998, **13**, 1238–1242.
14. Kraus, W. and Nolze, G., Powdercell2.4, Federal Institute for Materials Research and Testing Rudower Chaussee 5, 12489 Berlin, Germany.
15. Birajdar, D. S., Devatwal, U. N. and Jadhav, K. M., X-ray, IR and bulk magnetic properties of $Cu_{1+x}Mn_xFe_{2-2x}O_4$ ferrite system. *J. Mater. Sci.*, 2002, **37**, 1443–1448.
16. Buerger, M. J., *Crystal Structure Analysis*. Wiley, New York, 1960.